

Semi-Automatic Vessel Tracking and Segmentation Using Epicardial Ultrasound in Bypass Surgery

Alex Skovsbo Jørgensen¹, Samuel Emil Schmidt¹, Niels-Henrik Staalsen² and Lasse Riis Østergaard¹

Abstract—The purpose of intraoperative quality assessment of coronary artery bypass graft surgery is to confirm graft patency and disclose technical errors to reduce cardiac mortality, morbidity and improve clinical outcome for the patient. Epicardial ultrasound has been suggested as an alternative approach for quality assessment of anastomoses. To make a quantitative assessment of the anastomotic quality using ultrasound images, the vessel border has to be delineated to estimate the area of the vessel lumen. A tracking and segmentation algorithm was developed consisting of an active contour modeling approach and quality control of the segmentations. Evaluation of the tracking algorithm showed 91.96% of the segmentations were segmented correct with a mean error in height and width at 5.65% and 11.50% respectively.

I. INTRODUCTION

Coronary heart disease (CHD) is the most common cause of death worldwide [1]. Severe cases of CHD can be treated using coronary artery bypass graft surgery (CABG). In 2007 a total of 405.000 CABG procedures were made in the US, which makes it the most common surgical procedure [1]. Although CABG is viewed as a safe procedure, Mack et al. [2] has shown that up to 9% of anastomoses has a stenosis degree above 50%. Surgical errors can lead to early graft failure which can cause perioperative myocardial infarction, unfavorable long-term outcomes or fatal heart failure [3]. Therefore, an increased interest for quality assessment of anastomoses has been induced in recent years to disclose technical errors. It is presumed a significant portion of stenosed anastomoses can be corrected if surgical errors are detected by intraoperative anastomosis quality assessment [3]. That would improve the cost-effectiveness of CABG as the error can be corrected during the primary surgery [4].

The gold standard for anastomosis quality assessment is coronary angiography, but it is not normally available in the operation room and additional equipment and personnel are needed [3]. Therefore, other approaches have been advocated such as transit time flow measurement and intraoperative fluorescence imaging. These methods are simple, fast and safe but their sensitivity and specificity are low compared to coronary angiography and only work well at the extreme in determining graft patency [3]. Epicardial ultrasound (EUS) has been suggested as an alternative approach for intraoperative graft assessment [4], [5], [6]. To use EUS in clinical practice the anastomosis has to be evaluated on the beating

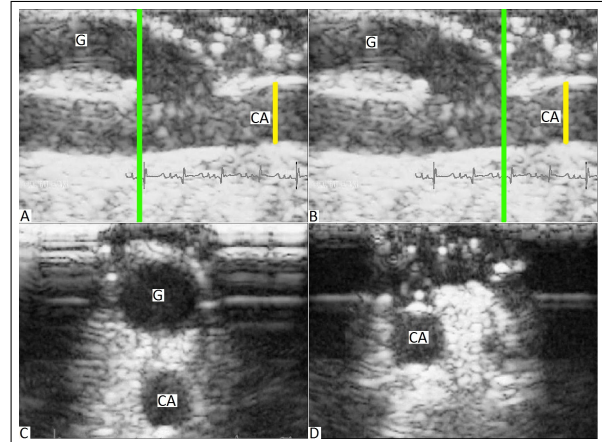


Fig. 1. Shows EUS images made using the Echoclip. A and B shows the longitudinal view of the anastomosis (G = graft, CA = coronary artery). C and D show the transverse view of the green line in A and B respectively, defined as the heel and toe of the anastomosis. The yellow line in A and B corresponds to the reference coronary artery distal to the anastomosis. In between the heel and toe is the midway heel/toe site of the anastomosis.

heart as it best represents the physiologic pressure and flow in the anastomosis. However imaging of the anastomotic site on the beating heart is difficult and prone to motion artifacts [4]. A novel ultrasound transducer positioning device, Echoclip [7] can limit gross motion of the vessels in the scan plane and obtain in vivo images of the anastomosis (fig. 1).

Currently EUS is not used routinely in clinical practice and has either been assessed qualitatively or by using off-line post-surgery analysis [4], [5], [6]. This is time consuming and users have to be trained in interpreting US images [4] which makes EUS unpractical to use during the primary surgery. However by developing an image analysis algorithm to track and segment the vessel borders through EUS sequences it may be possible to obtain a quantitative assessment of stenotic rates in anastomoses.

The stenotic rates of two specific surgical errors, the over sutured heel and toe, which impair the blood flow proximal and distal to the anastomosis respectively, can be assessed by comparing the area of the coronary artery in these landmarks to the area of a reference measurement of the coronary artery (fig. 1) [5]. Therefore by extracting the area of the coronary artery in these anastomotic sites through transverse EUS sequences a quantitative assessment of the stenosis degree can be obtained.

Previous studies have worked with tracking and segmentation of vessels in ultrasound images [8], [9], [10]. However the images of these studies have been obtained at different

¹Alex Skovsbo Jørgensen, Samuel Emil Schmidt, and Lasse Riis Østergaard are with the Department of Health Science and Technology, Aalborg University, Denmark

²Niels-Henrik Staalsen is with the Department of Cardiothoracic Surgery, Center for Cardiovascular research, Aalborg Hospital and Institute of Clinical Research, Skejby Sygehus, Aarhus University Hospital, Denmark

ultrasound frequencies which results in differences in image scale, resolution, and depth [10]. Also EUS sudden vessel movement in the scan plane can occur due to heart beats or small translations of the transducer which can impair the use of a priori knowledge of the vessel lumen movement.

This paper presents an algorithm for tracking and segmentation of the vessel lumen in in vivo EUS image sequences of porcine CABG end-to-side anastomoses using transverse images of the heel- and toe-sites.

II. TRACKING AND SEGMENTATION ALGORITHM

The tracking and segmentation algorithm is initialized manually by detecting a vessel center. A small contour is made around the vessel center and an initial snake is used to locate the vessel border. A multi scale snake is then used to make an accurate segmentation of the vessel as the preprocessing used in the initial snake decrease the accuracy in determining the vessel border. After each multi scale snake segmentation, the quality of the segmentation is assessed by a quality control step. If the segmentation is approved, the segmentation can be used to calculate the area of the vessel lumen. If the segmentation is not approved it is assumed the contour has not located the vessel border and the initial snake is used as a final segmentation in the frame. In frame $k+1$ an initial contour correction is made of the final segmentation in frame k to handle vessel translations in between frames and the multi scale snake is again used to segment the vessel lumen.

A. Initial- and Multi Scale Snake

The initial- and the multi scale snake are both active contours using an energy-minimizing spline (contour) guided by internal and external forces to evolve the contour to features of interest [11].

1) *Initial Snake*: The initial snake is used to locate the vessel wall when the contour is located far away from the image features of interest. This is the case when a vessel is detected in the first frame or if large vessel dilations occur in between frames. It is designed to expand until a sufficient amount of points on the contour lie in a significant image gradient. When using the initial snake it is assumed that the contour is located inside the vessel lumen. The energy formulation of the initial snake is [11], [12]:

$$\begin{aligned} E_{initial\ snake} &= \int_0^1 E_{elastic}\mathbf{v}(s) + E_{rigid}\mathbf{v}(s) \\ &\quad - E_{gradient}\mathbf{v}(s) - E_{area}\mathbf{v}(s)ds \\ &= \alpha|\mathbf{v}_i - \mathbf{v}_{i-1}|^2 + \beta|\mathbf{v}_{i+1} - 2\mathbf{v}_i + \mathbf{v}_{i-1}|^2 \\ &\quad - \gamma|G_\sigma * \nabla I(x, y)| - \kappa A \end{aligned} \quad (1)$$

where $\mathbf{v}(s)$ denote vertices on the contour, $'s'$ denotes the position on the contour by $0 \leq s \leq 1$ where 0 is the start and 1 is the end, $\alpha, \beta, \gamma, \kappa$ are weights of the respective energies (table I), G_σ is a Gaussian function of standard deviation σ , and ∇ is the gradient operator. The internal energies, $E_{elastic}$ and E_{rigid} , acts as contour constraints to prevent the contour

TABLE I
SHOW THE PARAMETERS USED FOR THE INITIAL SNAKE.

α	β	γ	κ
0.25	1	335	1

from moving through weak vessel borders and the parameters were determined to be between 0 and 1. $E_{elastic}$ is used to prefer extracting circular/ ellipsoid shapes of the contour and as vessels can have ellipsoid shapes a low α is chosen. E_{rigid} is used to prevent the contour from moving through missing vessel wall information e.g. when small branching vessels appear and therefore a high β is chosen. $E_{gradient}$ is the image feature used to extract the vessel borders. The feature image is filtered with a Gaussian low pass filter ($\sigma = 10$) to only extract large object regions and remove gradient information due to speckle inside the vessel lumen [11]. E_{area} use the area encapsulated by the contour as an inflation force. The sign of κ determine if the snake will expand or contract [12]. γ is chosen so $E_{gradient}$ can cancel out E_{area} in presence of a significant gradient.

2) *Multi Scale Snake*: The multi-scale snake use a coarse to fine approach using Gaussian low pass filters [14] to reduce the risk of locating false gradients when using the contour from frame k as the initial contour in frame $k+1$. To cope with vessel dynamics during the cardiac cycle in between frames when tracking a vessel it is designed to have no preference of inward or outward motion in the internal or external energies. The formulation of the multi scale snake is [11], [13], [14]:

$$\begin{aligned} E_{multi\ scale\ snake} &= \int_0^1 E_{eqDist}\mathbf{v}(s) + E_{rigid}\mathbf{v}(s) \\ &\quad - E_{multi\ scale\ gradient}\mathbf{v}(s)ds \\ &= \eta|\bar{d} - |\mathbf{v}_i - \mathbf{v}_{i-1}|| \\ &\quad + \beta|\mathbf{v}_{i+1} - 2\mathbf{v}_i + \mathbf{v}_{i-1}|^2 - \gamma|G_\sigma(\cdot; t) * \nabla I(x, y)| \end{aligned} \quad (2)$$

where \bar{d} is the average distance between points on the contour, $t>0$ denote scale and $\eta, \beta,$ and γ are weights of the respective energies (table II). The parameters of internal energies, E_{eqDist} and E_{rigid} , were determined to be between 0 and 1. E_{eqDist} encourage equal spacing of the contour points to make the snake more robust in capturing changes in shape of the vessel in between frames. A high η is chosen to keep the points on the contour as uniform as possible. E_{rigid} has the same function as in eq. 1. $E_{multi\ scale\ gradient}$ is the image feature used to segment the vessel border. To achieve a robust and accurate segmentation γ is reduced and β is increased from the coarse to fine scales as more spurious edges appear due to speckle in the fine scales.

The energy of the active contours is minimized using dynamic programming as in Amini et al. [15].

B. Quality Control

The quality control consists of a contour gradient analysis (CGA) where the mean gradient magnitude is calculated

TABLE II

SHOW THE PARAMETERS USED FOR THE MULTI SCALE SNAKE.

σ	η	β	γ
10	1	0.5	70
5	1	0.6	40
2	1	1	30
0	1	1	20

in four contour segments (left, right, top, and bottom). A robust CGA is obtained by interpolating the contour and use the gradient values in the contour points to calculate the mean gradient magnitude in each contour segment. If the mean gradient magnitude in a contour segment is below a threshold, ϖ , the segmentation is not approved. The gradient magnitude in the contour points are obtained from the gradient of an image filtered with a Gaussian low pass filter ($\sigma = 5$) to reduce gradient information due to speckle. ϖ is set to 2 which has been determined as a level of low vessel border information.

C. Initial Contour Correction

Even though the Echoclip minimizes gross motion of the vessels in the scan plane, translations of the vessels still occur in between frames due to the beating heart and small probe translations. Therefore an initial contour correction is made in each frame using a weighted centroid mean shift procedure (WCMS) to ensure the initial contour of the multi scale snake is located close to the vessel border in frame $k+1$. In WCMS the final contour in frame k is initialized at the same position in frame $k+1$. If a vessel translation occurs, bright intensities from the vessel wall and myocardium will appear inside the contour from frame k . Assuming the intensity content inside the vessel lumen is homogeneous, the contour from frame k is used as a spatial mask resembling a homogeneous area by computing the centroid (c) of the contour. In frame $k+1$ the vessel movement is estimated by computing the weighted centroid (wc) of the contour content and applying a mean shift procedure [16]:

$$\mathbf{v}(s)_{diff} = c\mathbf{v}(s) - wc\mathbf{v}(s) \quad (3)$$

The contour from frame k is moved according to $\mathbf{v}(s)_{diff}$ iteratively until $\mathbf{v}(s)_{diff}$ is less than a threshold, ϵ , which is set to an absolute movement of one pixel. The mean shift procedure will always converge to the local maximum homogeneous area when a part of the contour from frame k is located in the vessel lumen in frame $k+1$ [17].

III. SEGMENTATION EVALUATION

One end-to-side anastomosis was made in three anesthetized pigs that underwent CABG surgery. 10 EUS sequences were made of the heel and toe site in each anastomosis using a GE Vivid 4 echo machine (General Electric) and a 13-MHz, i13L GE ultrasound transducer (General Electric, Schenectady, NY) mounted in an Echoclip [7]. Each recording consisted of 40 - 112 frames (frame rate

TABLE IV

SHOW RESULTS FROM THE A POSTERIORI VISUAL VALIDATION OF SEGMENTATIONS APPROVED BY THE CGA.

Number of vessel segmentations	Approved segmentations	Failed segmentations	Error [%]
1544	1368	110	8.04

= 24 frames/second). Frames with occluded vessel wall information were excluded for the test.

To estimate the accuracy of the algorithm five vessel sequences were randomly selected. To obtain an independent assessment of the vessels 49 test frames were randomly selected from the five vessel sequences. As manual segmentation of the vessel lumen through an EUS sequence is a tedious task and prone to inter- and intra-observer variability a fast and simple estimate of the segmentation accuracy was made where an expert user determined the vessel height and width by placing a bounding box around the vessels in the test frames. The tracking and segmentation algorithm was used on each vessel sequence and a bounding box was obtained of the segmentations approved by the quality control. Frames with non-approved segmentations was discarded from the test. In the remaining frames the mean width and height of the vessels assessed by the expert was calculated. Then the mean error in percent and root mean square (RMS) value of the differences in width and height of the bounding boxes of the expert and the segmentation was found.

To supplement the quantitative accuracy test 22 vessel sequences (14 toe- and 4 heel-view) were randomly chosen for a qualitative evaluation of the segmentations in the sequences. In each sequence the tracking and segmentation algorithm was used to segment the vessels in a total of 1544 vessel segmentations. A manual a posteriori visual validation of the segmentations approved by the quality control was made by a non-expert to determine the number of failed segmentations, defined as segmentations that over- or underestimated the vessel lumen.

IV. RESULTS

An example of three vessel segmentations can be seen in fig. 2. The results of the quantitative accuracy test can be seen in table III. The mean error in height and width of the segmentations was 5.65% and 11.50% respectively which indicates the algorithm is less accurate in locating vessel borders that lie parallel to the ultrasound waves. The results of the qualitative a posteriori visual validation can be seen in table IV. 88.60% of all vessel segmentations were approved by the quality control and 91.96% of these segmentations were assessed as correct.

V. DISCUSSION

We have presented a segmentation and tracking framework to delineate vessel borders of CABG anastomoses in in vivo EUS sequences. It has been shown that it is possible

TABLE III
SHOW THE RESULTS OF THE QUANTITATIVE ACCURACY TEST.

Vessels selected	Approved segmentations	Mean width [pixels]	Mean height [pixels]	RMS error width [pixels]	RMS error height [pixels]	Mean error width [%]	Mean error height [%]
90	74	147.72	146.84	22.59	10.93	11.50	5.65

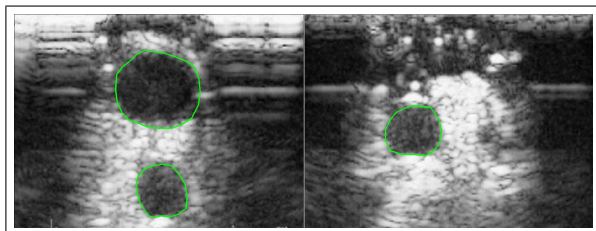


Fig. 2. Examples of vessel segmentations in the heel- and toe-view.

to track and segment vessels with a low error rate in the segmentations approved by the quality control.

It was observed that segmentation errors mainly occurred when the vessel border information was low either due to anisotropy or if sufficient vessel border information was not provided by the operator of the transducer e.g. if the vessel border was located close to the lateral limit of the acoustic range causing a reduction in vessel border intensity. In both cases the quality control may assess the quality of the segmentation as low and use the initial snake leading to an over estimation of the vessel lumen. Instead the quality control may be used to discard frames where no improvement in the gradient information is observed after the use of the initial snake as erroneous measurements will bias the estimation of the vessel lumen area.

The parameters of the snakes were determined using a combination of determining the ratio of the internal energies based on knowledge of the anatomy and empirical testing with the external energies. In the empirical testing we did not experience any significant changes in segmentation accuracy when making minor changes in the parameters. However, as the external energies are mainly contrast based, an improvement in the results may be obtained by fitting the external parameters according to the intensity content inside the vessel lumen.

Clinical grading of stenosis degrees has to be viewed in the context that the golden standard, coronary angiography, has shown a significant interobserver variability in determining the diameter stenosis [18]. Therefore the current framework is expected to add detail of stenotic rates compared to the current stenotic rate grading using the FitzGibbon grading system where a clinical significant stenosis is defined by a vessel diameter reduction threshold of 50% in one of six scan planes of the anastomosis.

ACKNOWLEDGMENT

Thanks to Spar Nord Fonden for financial support of the project.

REFERENCES

- [1] M. J. Hall, C. J. DeFrances S. N. Williams A. Golosonskiy and A. Schwartzman, National Hospital Discharge Survey: 2007 Summary, National Health Statistics Report, no. 29, 2010, pp. 1-20.
- [2] M. J. Mack, J. A. Magovern, T. A. Acuff, R. J. Landreneau, D. M. Tennon, E. J. Tinnerman and J. A. Osborne, Results of graft patency by immediate angiography in minimally invasive coronary artery surgery, *Ann Thorac Surg*, vol. 68, 1999, pp. 383-389.
- [3] M. J. Mack, Intraoperative coronary graft assessment, *Curr Opin Cardiol*, vol. 23, 2008, pp. 568-572.
- [4] R. P. J. Budde, R. Meijer, T. C. Dessing, C. Borst and P. F. Gründeman, Detection of construction errors in ex vivo coronary artery anastomoses by 13-MHz epicardial ultrasonography, *J Thorac Cardiovasc Surg*, vol. 129, 2005, pp. 1078-1083.
- [5] T. C. Dessing, R. P. J. Budde, R. Meijer, P. F. A. Bakker, C. Borst and P. F. Gründeman, Geometry assessment of coronary artery anastomoses with construction errors by epicardial ultrasound, *European Journal of Cardio-thoracic Surgery*, vol. 26, 2004, pp. 257-261.
- [6] I. S. Khalid, L. Løvstakken, I. Kirkeby-Garstad, H. Torp, H. Vik-Mo and R. Haaverstad: Effect of the cardiac cycle on the coronary anastomosis assessed by ultrasound. *Asian Cardiocasc Thorac Ann*, vol. 15, 2007, 86-90
- [7] N.-H. Staalsen, B. Kjaergaard and J. J. Andreasen, A new technique facilitating intraoperative high-frequency echocardiography of coronary bypass graft anastomoses, *The journal of thoracic and cardiovascular surgery*, vol. 141, no. 1, 2011, pp. 295-296.
- [8] J. Guerrero, S. E. Salcudean, J. A. McEwen, B. A. Masri and S. Nicolaou, Real-time vessel segmentation and tracking for ultrasound imaging applications, *IEEE Transactions on Medical Imaging*, vol. 26, no. 8, 2007, pp. 1079-1090.
- [9] E. Brusseau, C. L. de Korte, F. Mastik, J. Schaar and A. F. W. van der Steen, Fully automatic luminal contour segmentation in intracoronary ultrasound imaging - a statistical approach, *IEEE Transactions on Medical Imaging*, vol. 23, no. 5, 2004, pp. 554-566.
- [10] M. C. Moraes and S. S. Furuic, Wall Segmentation in Intravascular Ultrasound Images Using Binary Morphological Reconstruction, *Ultrasound Med Biol*, vol. 37, no. 9, 2011, pp. 1486-1499.
- [11] M. Kass, A. Witkin and D. Terzopoulos, Snakes: Active contour models, *International journal of computer vision*, vol. 1, no. 4, 1988, pp. 321-331.
- [12] L. Cohen and I. Cohen, Finite element methods for active contour models and balloons for 2d and 3d images, *IEEE transaction on pattern analysis and machine intelligence*, vol. 15, no. 11, 1993, pp. 1131-1147.
- [13] L. Ji and H. Yan, Attractable snakes based on the greedy algorithm for contour extraction, *Pattern Recognition*, vol. 35, 2002, pp. 791-806.
- [14] T. Lindeberg and B. M. H. Romeny, *Linear Scale-Space, Geometry-Driven Diffusion in Computer Vision*, Pearson Education Inc., 1994, pp. 1-41.
- [15] A. Amini, T. E. Weymouth and R. C. Jain, Using dynamic programming for solving variational problems in vision, *IEEE transaction on pattern analysis and machine intelligence*, vol. 12, no. 9, 1990, pp. 855-867.
- [16] K. Fukunaga and L. D. Hostetler, The estimation of the gradient of a density function with applications in pattern recognition, *IEEE trans. information theory*, vol. 21, no. 1, 1975, pp. 32-40.
- [17] D. Comaniciu, V. Ramesh and P. Meer, Kernel-based object tracking, *IEEE transaction on pattern analysis and machine intelligence*, vol. 25, no. 5, 2003, pp. 564-577.
- [18] G. J. Beaman and R. A. Vogel, Accuracy of individual and panel visual interpretations of coronary arteriograms: implications for clinical decisions, *J am Coll Cardiol*, vol. 16, 1990, pp. 108-113.